

Market-Clearing With Stochastic Security— Part II: Case Studies

François Bouffard, *Student Member, IEEE*, Francisco D. Galiana, *Fellow, IEEE*, and Antonio J. Conejo, *Fellow, IEEE*

Abstract—This paper analyzes the market-clearing formulation with stochastic security developed in its companion paper through two case studies solved using mixed-integer linear programming techniques. The generation and reserve schedules as well as the nodal prices of energy and security are assessed under various conditions such as *a)* line flow limits, *b)* when nonspinning reserve is excluded from the formulation, *c)* demand-side valuation of energy not served, *d)* generator ramping limits, and *e)* the set of pre-selected contingencies.

Index Terms—Computational complexity, electricity markets, expected load not served, marginal pricing, mixed-integer linear programming, reserve, security, stochastic unit commitment, value of lost load.

NOMENCLATURE

For a listing of the symbols used here, we refer the reader to the companion paper [1].

I. INTRODUCTION

THIS paper analyzes the market-clearing formulation with stochastic security developed in its companion paper [1] through two case studies solved using mixed-integer linear programming techniques.

In Section II, a three-bus, three-line, three-generator system scheduled over a four-hour horizon is studied in depth. This case is simple enough so that the correctness of the results can be readily verified, yet it conveys many interesting features of the proposed market-clearing formulation. Thus, in this case, we examine the effects of *a)* line flow limits, *b)* opportunity cost of excluding nonspinning reserve in the formulation, *c)* demand-side valuation of energy not served, *d)* ramping limits, and *e)* the pre-selected set of contingencies. Furthermore, we derive and assess the nodal prices of energy and security.

In Section III, the IEEE Reliability Test System (IEEE RTS) [2] is scheduled over a 24-h horizon. This case brings out some of the dimensionality issues of the proposed scheme.

Manuscript received December 20, 2004; revised June 10, 2005. This work was supported by the Natural Sciences and Engineering Research Council of Canada, by the Fonds québécois de la recherche sur la nature et les technologies and by the Ministry of Science and Technology of Spain, CICYT DPI 2003-01362. Paper no. TPWRS-00659-2004.

F. Bouffard and F. D. Galiana are with the Department of Electrical and Computer Engineering, McGill University, Montreal, QC H3A 2A7, Canada (e-mail: francois.bouffard@mcgill.ca; galiana@ece.mcgill.ca).

A. J. Conejo is with the Department of Electrical Engineering, Universidad de Castilla-La Mancha, Ciudad Real 13071, Spain (e-mail: antonio.conejo@uclm.es).

Digital Object Identifier 10.1109/TPWRS.2005.857015

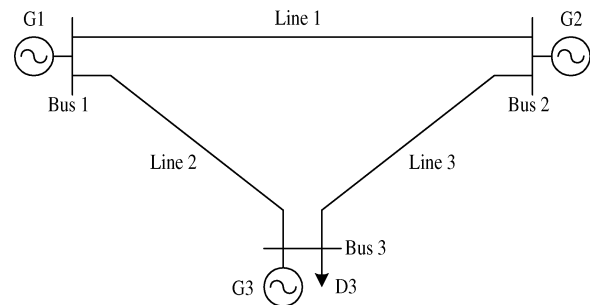


Fig. 1. Three-bus, three-line, three-generator power system.

TABLE I
HOURLY DEMAND PROFILE AT BUS 3 (MW)

	Time t (h)			
	1	2	3	4
d_{3t}	30	80	110	40

TABLE II
GENERATOR DATA

	Generator i		
	1	2	3
g_i^{\min} (MW)	10	10	10
g_i^{\max} (MW)	100	100	50
a_{it} (\$/MWh)	30.00	40.00	20.00
c_i^{su} (\$/h)	100.00	100.00	100.00
\tilde{q}_{it}^{up} (\$/MWh)	5.00	7.00	8.00
\tilde{q}_{it}^{dn} (\$/MWh)	5.00	7.00	8.00
\tilde{q}_{it}^{up} (\$/MWh)	4.50	5.50	7.00
\tilde{q}_{it}^{dn} (\$/MWh)	4.50	5.50	7.00
λ_i^{-1} (h)	500	500	250

II. SMALL-SCALE STUDY

This case study analyzes the scheduling of the power system in Fig. 1 over four consecutive hours. The three lines have identical admittance, maximum power carrying capacity of 55 MW, and mean time to failure of 10 000 h.

An inelastic demand is located at bus 3 and varies hour by hour according to the pattern detailed in Table I. In addition, the consumer at bus 3 offers up to 10% of the hourly load as spinning reserve services (both up- and down-going) at the rate of \$20 per megawatthour. We assume as well that this consumer values involuntary loss-of-load at the rate of \$1000 per megawatthour during all four hours.

The generating unit data are found in Table II. The energy and reserve offers of the generators remain unchanged for all hours of the scheduling horizon. In this example, the generators do

not incur fixed operating costs other than the startup costs c_i^{su} . Each generator offers a single block of energy ranging between its technical minimum g_i^{\min} and maximum g_i^{\max} at the rate of a_{it} dollars per megawatthour. Likewise, the bounds on the amounts of reserve services offered are set to be the largest possible, in other words, the upper bound on up and down spinning reserve is $g_i^{\max} - g_i^{\min}$ and for nonspinning reserves it is equal to g_i^{\max} . The generation-side reserve services are offered at rates, in dollars per megawatthour, shown in Table II as q_{it}^{up} for up-going spinning reserve, q_{it}^{dn} for down-going spinning reserve, \tilde{q}_{it}^{up} for up-going nonspinning reserve, and \tilde{q}_{it}^{dn} for down-going nonspinning reserve. Finally, the last row of Table II lists the mean times to failure (λ_i^{-1}) of each of the generators.

In this example, for the sake of simplicity, the generator minimum up and down time constraints are assumed to be inactive, and their ramping capabilities are set to g_i^{\max} megawatts per hour, in other words, the maximum generation capacity. Finally, we assume that all three generators are in the off state at time $t = 0$.

The set of pre-selected contingencies characterizing the security criterion comprise all single generator and line outages. We use the indexes $k = \{1, 2, 3\}$ to represent the failure of generators 1, 2, and 3, respectively, while $k = \{4, 5, 6\}$ index the failure of lines 1, 2, and 3, respectively; each of these six contingencies can occur in any of the four hours of the scheduling horizon. Notice that the $6 \times 4 = 24$ contingency scenarios characterizing the security criterion in this problem are relatively few compared to all possible contingency scenarios. The latter is defined by all combinations of generator and line outages over all possible times of occurrence, including nonsimultaneous failures, which in this example equals $\sum_{n=1}^6 4^n \binom{6}{n} = 15624$.

For the given data, the stochastic market-clearing formulation is already in linear form. It was solved using CPLEX 9.0.0, a mixed-integer linear programming solver under GAMS [3]. Computation times were all less than one second on a PC equipped with a 1.80-MHz Pentium 4 processor and 512 MB of RAM.

A. Results and Analysis

Tables III and IV summarize the key features of the optimal schedule obtained. Table III gives the breakdown of the corresponding expected cost. Not surprisingly, the component corresponding to the expected operating cost under no contingencies is dominant with 95.01% of the total amount. What remains are the expected costs incurred following the occurrence of the pre-selected contingencies, an amount split between the expected cost of deploying the reserves by re-dispatching and turning on generators (3.30% of the total) and the expected cost incurred by the consumers due to involuntary load shedding (1.69% of the total).

This breakdown is consistent with the probability level that none of the pre-selected contingencies occurs, $p_0 = 0.9673$, an amount which is close to its associated expected cost proportion (95.01%). Likewise, the expected costs' percentages associated with reserve deployment and load shedding ($3.30 + 1.69 = 4.99\%$) are of the same order of magnitude

TABLE III
BREAKDOWN OF EXPECTED COSTS

	Total	Pre-contingency	Reserve deployment	Loss-of-load
Cost (\$)	7228.74	6868.15	238.51	122.07
% total cost	100.00	95.01	3.30	1.69

TABLE IV
POWER (MW), RESERVES (MW), AND ELNS (MWH)

	Time t (h)			
	1	2	3	4
g_{1t}	0	30	60	0
r_{1t}^{up}	0	20	0	0
r_{1t}^{dn}	0	0	5	0
\tilde{r}_{1t}^{up}	0	0	0	40
\tilde{r}_{1t}^{dn}	0	0	0	0
g_{2t}	0	0	0	0
r_{2t}^{up}	0	0	0	0
r_{2t}^{dn}	0	0	0	0
\tilde{r}_{2t}^{up}	0	30	60	0
\tilde{r}_{2t}^{dn}	0	0	0	0
g_{3t}	30	50	50	40
r_{3t}^{up}	0	0	0	0
r_{3t}^{dn}	0	0	0	0
\tilde{r}_{3t}^{up}	0	0	0	0
\tilde{r}_{3t}^{dn}	0	0	0	0
d_{3t}	30	80	110	40
r_{3t}^{up}	0	0	0	0
r_{3t}^{dn}	0	0	0	0
$ELNS_{3t}$	0.1177	0	0.0044	0

as the sum of the probabilities of the contingency scenarios $\sum_{k,\tau} p(k,\tau) = 0.0323$.

Table IV outlines the optimal generation and reserve schedules of the generators as well as the demand reserve contributions. Generator 3, being incrementally the cheapest (\$20/MWh), supplies power during all the four hours but does not provide any reserve. Generator 1, being the next cheapest unit (\$30/MWh), picks up the residual demand during the peak periods 2 and 3. In addition, generator 1 provides nonspinning up reserve during hour 4, up-spinning reserve during period 2, and down-spinning reserve during period 3. Generator 2, costing \$40/MWh, is never turned on but provides nonspinning reserve during periods 2 and 3. The load at bus 3 does not provide any voluntary reserve; however, as seen in the last row of Table IV, the optimum market-clearing schedule calls for some involuntary load shedding during periods 1 and 3. We also observe from the table that due to the high value of lost load (\$1000/MWh), the ELNS at bus 3 over the horizon is relatively low, equaling 0.1221 MWh, or 0.05% of the 260 MWh of energy consumed over the four hours.

What makes this last result particularly interesting is that in spite of its high cost, the market-clearing solution still calls for some amount of load shedding. This brings out the essence of stochastic security, which considers simultaneously the credibility and severity of the contingencies making up the security criterion.

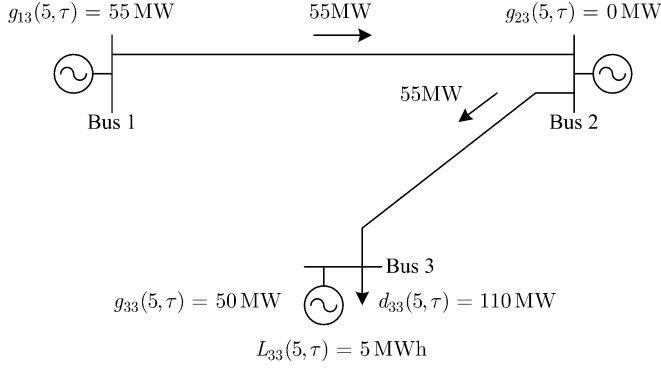


Fig. 2. Effect of the outage of line 2 ($k = 5$) during period $t = 3$ if it occurs during $\tau \in \{1, 2, 3\}$.

Next, referring to Table IV, we analyze in detail how reserve levels are set during each time period and particularly how and why load is shed under the stochastic market-clearing solution.

Period $t = 1$: We observe, perhaps surprisingly, that during this period, no reserve is scheduled, and, as a consequence, the loss of generator 3 would not be covered. This result is unique to the stochastic market-clearing approach, reflecting the fact that the loss of generator 3 has both a low probability and a low impact in light of the relative expected costs of reserve deployment and load shedding. In fact, this contingency would be covered only if the value of lost load were raised over \$1171/MWh for that hour. The loss of the other generators or lines do not cause loss-of-load during period 1.

Period $t = 2$: The loss of generator 1 occurring during the periods $\tau \in \{1, 2\}$ is covered by the 30 MW of nonspinning up reserve provided by generator 2. Likewise, the loss of generator 3 is covered by the 20 MW of up-spinning reserve of generator 1 and the 30 MW of nonspinning reserve of generator 2. None of the line losses occurring during $\tau \in \{1, 2\}$ cause loss-of-load.

Period $t = 3$: The loss of generator 1 during one of $\tau \in \{1, 2, 3\}$ is fully covered by the nonspinning up reserve provided by generator 2 (60 MW). When generator 3 is lost during one of $\tau \in \{1, 2, 3\}$, generator 1 needs to back down by 5 MW (explaining its provision of 5 MW of down-spinning reserve), while generator 2 turns on to provide 55 MW from its nonspinning reserve up provision. Thus, the involuntary load loss associated with this contingency is nil during that hour. This post-contingency dispatch maximizes the use of the transmission network to minimize the amount of load shed at bus 3. If generator 1 were to keep producing at the pre-contingency level of 60 MW, then generator 2 would only be able to deliver 45 MW because of the line flow limits of 55 MW. This situation would lead to a loss-of-load of 5 MWh at bus 3.

All the line outages occurring during one of $\tau \in \{1, 2, 3\}$ lead to load shedding of 5 MWh during that hour because the low probabilities and the low expected impacts associated with these events do not warrant that they be fully covered with reserve. Fig. 2 shows an example of how reserves are deployed after the loss of line 2. Here generator 1 needs to back down by 5 MW to comply with the line flow limitations, with generator 2 staying off and generator 3 operating at 50 MW.

Period $t = 4$: The loss of generator 3 during either $\tau \in \{1, 2, 3, 4\}$ is covered by the 40 MW of up-going nonspinning

TABLE V
POWER AND RESERVES (MW)—DETERMINISTIC

	Time t (h)			
	1	2	3	4
g_{1t}	0	30	60	0
r_{1t}^{up}	0	20	0	0
r_{1t}^{dn}	0	0	5	0
\tilde{r}_{1t}^{up}	30	0	0	40
\tilde{r}_{1t}^{dn}	0	0	0	0
g_{2t}	0	0	0	0
r_{2t}^{up}	0	0	0	0
r_{2t}^{dn}	0	0	0	0
\tilde{r}_{2t}^{up}	0	30	55	0
\tilde{r}_{2t}^{dn}	0	0	0	0
g_{3t}	30	50	50	40
r_{3t}^{up}	0	0	0	0
r_{3t}^{dn}	0	0	0	0
\tilde{r}_{3t}^{up}	0	0	0	0
\tilde{r}_{3t}^{dn}	0	0	0	0
d_{3t}	30	80	110	40
r_{3t}^{up}	0	0	5	0
r_{3t}^{dn}	0	0	0	0

reserve provided by generator 1. None of the single line outages occurring during one of $\tau \in \{1, 2, 3, 4\}$ create loss-of-load. Likewise, outages affecting generator 1 or 2 do not cause loss-of-load.

B. Stochastic Versus Deterministic Schedules

It is of interest to compare the results obtained with the stochastic approach to those of a purely deterministic security-constrained schedule where load shedding is not permitted. Table V shows that in the deterministic case, generator 1 gets to provide an extra 30 MW of up-going nonspinning reserve during the first hour to cover the loss of generator 3. Moreover, during period $t = 3$, the load is scheduled to provide 5 MW of up-going spinning (voluntary) reserve to cover the losses of lines. Note as well that this 5 MW is used following the outage of generator 1 or 3 occurring during $\tau \in \{1, 2, 3\}$. This explains why generator 2 provides 55 MW of up-going nonspinning reserve during period $t = 3$ instead of the 60 MW seen in Table IV. Therefore, the loss of generator 1 (60 MW), for instance, would be compensated by 55 MW coming from generator 2 added to the 5 MW from the voluntary reduction in demand at bus 3. However, we must point out that the cost incurred to schedule these 5 MW of demand-side reserve during $t = 3$ (\$100) is much higher than the expected cost of load shedding (\$4.40) given the value of lost load (\$1000/MWh) and the outage probabilities.

Table VI compares the breakdown of the expected cost of the stochastic schedule to the expected cost of the deterministic schedule, given by the expression

$$p_0 C_{det}^* + \sum_{\tau=1}^T \sum_{k=1}^K p(k, \tau) C_{det}^*(k, \tau). \quad (1)$$

In this relation C_{det}^* is the optimal cost of the deterministic schedule, and $C_{det}^*(k, \tau)$ are the reserve deployment costs

TABLE VI
COMPARISON OF EXPECTED COSTS (\$)—DETERMINISTIC VERSUS STOCHASTIC

	Pre-contingency	Reserve deployment	Loss-of-load
Deterministic	7068.87	240.51	0.00
Stochastic	6868.15	238.51	122.07
Difference	200.72	2.00	-122.07

associated with the contingency scenarios being considered. The term $p_0 C_{det}^*$ denotes the expected cost incurred in the event that no contingencies occur, while the terms $p(k, \tau) C_{det}^*(k, \tau)$ correspond to the expected costs incurred when deploying the reserves under contingency scenario (k, τ) . Table VI demonstrates that the “Pre-contingency” and the “Reserve deployment” expected costs of the stochastic schedule are lower than those associated with the deterministic schedule. However, the expected costs associated with load shedding in the stochastic schedule diminishes these gains. The efficiency gain of the stochastic programming solution versus that of the deterministic solution is known as the value of the stochastic solution (VSS) [4], which, in this case, equals $\$200.72 + \$2.00 - \$122.07 = \80.65 . This result illustrates that when one considers the probabilities of failure, it is possible to pre-position the system more economically, while still achieving a high level of security on the average.

C. Prices of Energy and Security

In addition to the market-clearing procedure defined in the companion paper, it is also necessary to specify a set of pricing rules such as locational marginal pricing [5], which has gained industry acceptance and is now widely used [6].

Recent research on security-constrained electricity market-clearing problems [7] argues further that *all* the reserve services supplied at a bus should be priced at the corresponding nodal marginal cost of security. The core argument in favor of a single per-bus price for all reserve services stems from the fact that in ensuring the security of the energy supply, *all* the reserve services act in a concerted manner. In this paper, we use the marginal pricing rules of [7] summarized in the Appendix. This proposition contrasts with current practices in which different reserve services—up/down and spinning/nonspinning reserves—are priced at different marginal rates [8]–[11].

The first three rows of Tables VII and VIII list the nodal prices of security and energy for the stochastic formulation schedule. We observe the presence of nodal price differences during the third period as a consequence of line congestion following the random failure of any one of the lines.

It is also of interest to compare the nodal prices between the deterministic and stochastic market-clearing formulations. Note, however, that this comparison cannot be readily done because the sets of prices corresponding to the deterministic market-clearing would be derived from an optimization problem with a different objective function. Thus, to unbiased the comparison, we computed the corresponding deterministic prices of security and energy from the expected cost of the deterministic schedule (1) from small perturbations of the power balance

TABLE VII
PRICES OF SECURITY (\$/MWH)

		Time t (h)			
		1	2	3	4
		Stochastic Schedule			
Bus	1	8.1108	6.0122	1.2739	12.8939
	2	8.1108	6.0122	6.8225	12.8939
	3	8.1108	6.0122	7.2300	12.8939
		Deterministic Schedule			
Bus	1	12.6000	6.0100	1.7100	12.9000
	2	12.6000	6.0100	19.6600	12.9000
	3	12.6000	6.0100	19.3500	12.9000

TABLE VIII
PRICES OF ENERGY (\$/MWH)

		Time t (h)			
		1	2	3	4
		Stochastic Schedule			
Bus	1	23.8384	30.5984	35.4124	24.5020
	2	23.8384	30.5984	40.9610	24.5020
	3	23.8384	30.5984	41.3685	24.5020
		Deterministic Schedule			
Bus	1	24.5000	30.6000	35.4100	24.5000
	2	24.5000	30.6000	53.3700	24.5000
	3	24.5000	30.6000	53.4900	24.5000

relations in the deterministic formulation. That is, the nodal prices of energy for the deterministic schedule in Table VIII are equal to the ratios of the increments in the expected cost of the deterministic schedule from small nodal demand increments affecting both the pre- and post-contingency power balance relations to the corresponding demand increments. Likewise, the deterministic nodal prices in Table VII were calculated from the same principle but, this time, only perturbing the post-contingency power balance relations.

Comparing the first three rows of Table VII to the last three rows of that table, we observe that during periods 1 and 3, when load shedding is used in the stochastic solution, the stochastic prices of security are much lower than the those of the deterministic schedule. During the remaining periods, the corresponding prices of security are nearly identical. This demonstrates once more that in this example, it is incrementally cheaper on average to shed load than to schedule and deploy incrementally more expensive reserves.

Comparing the prices of energy in Table VIII, we find again that the stochastic prices are generally lower than those of the deterministic case. Like in the case of the prices of security, we remark that during periods 1 and 3, the stochastic prices of energy are lower than those corresponding to the deterministic schedule. For example, the price of energy corresponding to the stochastic schedule seen by the consumers at bus 3 during period 3 is 23% lower on average than that corresponding to the deterministic schedule. Such prices differences, thus, reflect premiums assumed by the consumers for risking involuntary load shedding.

TABLE IX
BREAKDOWN OF EXPECTED COSTS—EXCLUDING NONSPINNING RESERVE

	Total	Pre-contingency	Reserve deployment	Loss-of-load
Excluding nonspinning reserve				
Cost (\$)	7721.07	7148.68	228.13	344.26
% total cost	100.00	92.59	2.95	4.46
With nonspinning reserve				
Cost (\$)	7228.74	6868.15	238.51	122.07
% total cost	100.00	95.01	3.30	1.69
Diff. (\$)	492.33	280.53	-10.38	222.19
Diff. (%)	6.38	4.08	-4.35	182.00

TABLE X
POWER (MW), RESERVES (MW), AND ELNS (MWh)
—EXCLUDING NONSPINNING RESERVE

	Time t (h)			
	1	2	3	4
g_{1t}	0	30	50	10
r_{1t}^{up}	0	50	10	30
r_{1t}^{dn}	0	0	5	0
g_{2t}	0	0	10	0
r_{2t}^{up}	0	0	45	0
r_{2t}^{dn}	0	0	0	0
g_{3t}	30	50	50	30
r_{3t}^{up}	0	0	0	0
r_{3t}^{dn}	0	0	0	0
d_{3t}	30	80	110	40
r_{3t}^{up}	0	0	0	0
r_{3t}^{dn}	0	0	0	0
$ELNS_{3t}$	0.1177	0.1168	0.0321	0.0777

D. Impact of Some Key Parameters

1) *Nonspinning Reserve*: The inclusion of nonspinning reserve in the market-clearing formulation requires the optimization of the on/off generation status for all contingency scenarios. This is a feature that for large systems leads to computational intractability [1].

We have, therefore, examined the impact of ignoring nonspinning reserve with the current small system. The first two rows of Table IX show the breakdown of the expected costs without nonspinning reserve. Comparing these results with the cost breakdown with nonspinning reserve in the next two rows, we see that the expected cost components have increased without nonspinning reserve. However, the expected cost associated with post-contingency reserve deployment has gone down by 4.35% because now this component does not include start-up costs. In contrast, the expected cost of loss-of-load has jumped up by a significant 182%. This increase is better explained by looking at the reserves and generation schedules shown in Table X. Here the loss of generator 1 is not covered during period 2, thus causing a 30-MWh loss-of-load, unlike previously, where generator 2 was providing 30 MW of nonspinning reserve.

This is a good example of the tug of war between security and economics. In fact, it can be shown that if the value of lost load is raised to \$1247/MWh in the case with spinning reserve

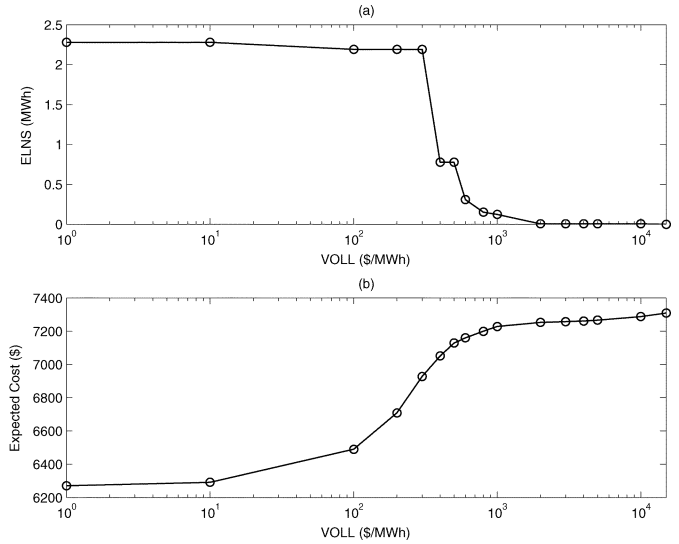


Fig. 3. Effect of the magnitude of the value of lost load at bus 3. (a) On the ELNS. (b) On the total expected cost.

only, then the ELNS can be reduced back to the level found in the case with nonspinning reserve (0.1221 MWh). This improvement in security, however, comes at a cost, principally by increasing the expected cost of pre-contingency operation to \$7395.35 from \$6868.15 and the expected cost of reserve deployment to \$241.27 from \$238.51.

2) *Value of Lost Load*: We saw from the previous section that raising the value of lost load (VOLL) can improve the security of supply in the sense of ELNS but that this comes at a cost. Fig. 3 shows how the ELNS and the total expected cost vary with VOLL. We observe that ELNS is initially relatively insensitive to VOLL with a slight tendency to decrease monotonically, with a sharp decline in the range between \$300/MWh and \$1000/MWh. It is at these levels that the expected cost of load shedding begins to be significant compared to the expected cost of reserve deployment.

3) *Ramping Limits*: The effects of ramping limitations constitute a prime concern in time-dynamic generation scheduling problems, especially those with reserve constraints. So far, in this case study, the generators were not constrained by ramp limits because we assumed that they could ramp from zero to g_i^{\max} and vice versa within a period.

Now we assume that generator 1 has a ramping limitation of 29 MW/h, while generators 2 and 3 can still change their output at the rates of 100 and 50 MW/h, respectively. These rates apply for up- and down-going ramping, including startup and shutdown ramps.

Comparing Table XI to Table IV, we observe significant changes in the schedule due to the ramping limitations of generator 1. A noticeable difference is the requirement that generator 2 be turned on during the third period. Moreover, the ramp limitations impede generator 1 from turning off during the fourth period; this, as a result, forces generator 3 to back off by the 21 MW that generator 1 has to produce. Another interesting point is the scheduling of 2.5 MW of demand-side reserve during the interval $t = 3$. This reserve, costing \$20/MWh, is used most notably to avoid deploying the reserve of generator

TABLE XI
POWER (MW), RESERVES (MW), AND ELNS (MWH)—RAMP LIMITS

	Time t (h)			
	1	2	3	4
g_{1t}	10	30	50	21
r_{1t}^{up}	0	9	0	0
r_{1t}^{dn}	0	0	5	0
r_{1t}^{up}	0	0	0	0
r_{1t}^{dn}	0	0	0	0
g_{2t}	0	0	10	0
r_{2t}^{up}	0	0	47.5	0
r_{2t}^{dn}	0	0	0	0
r_{2t}^{up}	10	41	0	21
r_{2t}^{dn}	0	0	0	0
g_{3t}	20	50	50	19
r_{3t}^{up}	0	0	0	0
r_{3t}^{dn}	0	0	0	0
r_{3t}^{up}	0	0	0	0
r_{3t}^{dn}	0	0	0	0
d_{3t}	30	80	110	40
r_{3t}^{up}	0	0	2.5	0
r_{3t}^{dn}	0	0	0	0
$ELNS_{3t}$	0.0392	0	0.0452	0

TABLE XII
ELNS (MWH) UNDER ALTERNATE SET OF CONTINGENCIES

	Time t (h)			
	1	2	3	4
	Alternate set of contingencies			
$ELNS_{3t}$	0.1182	0.0015	0.0074	0.0013
	Original set of contingencies			
$ELNS_{3t}$	0.1177	0.0000	0.0044	0.0000

2 into actual energy production (at the rate of \$40/MWh) following the loss of a line.

4) *Set of Pre-Selected Contingencies:* The choice of the pre-selected contingencies can have significant effects. For example, by adding a new contingency to an already existing set, the probability that no contingency occurs, p_0 , decreases, while the probability that at least one contingency occurs, $\sum_{k,\tau} p(k,\tau)$, increases. As a result, the pre-contingency expected welfare term proportional to p_0 will generally carry less weight. The reserve deployment expected cost term, however, is affected more significantly, since the objective function must now account for the extra expected cost. Furthermore, it may happen that the new contingency requires more load shedding if its associated expected cost increment is smaller than that of reserve deployment. However, the addition of one more contingency to the existing pre-selected set cannot worsen the value of the *true* ELNS, which considers all possible contingency scenarios.

To illustrate the above statements, consider the addition of all double generator outages (assumed to occur independently and simultaneously) to the original set of pre-selected contingencies. The optimal stochastic generation and reserve schedule is still identical to the one in Table IV; however, all the levels of ELNS have now increased as seen in Table XII (for a total of 0.1236 MWh over the horizon). The small increments in ELNS

TABLE XIII
BREAKDOWN OF EXPECTED COSTS—ALTERNATE SET OF CONTINGENCIES

	Total	Pre-contingency	Reserve deployment	Loss-of-load
	Alternate set of contingencies			
Cost (\$)	6913.54	6546.27	238.92	128.36
% total cost	100.00	94.69	3.46	1.86
	Original set of contingencies			
Cost (\$)	7228.74	6868.15	238.51	122.07
% total cost	100.00	95.01	3.30	1.69

caused by the extra contingencies did not warrant scheduling more reserve. This example demonstrates that, when using stochastic market-clearing, new contingencies are not necessarily fully covered in the deterministic sense (in fact, a deterministic market-clearing would be infeasible in this case). In stochastic market-clearing, when considering extra contingencies, additional reserve is scheduled only if the expected cost of reserve scheduling and, especially, deployment is less than the expected cost of load shedding.

Finally, comparing the expected cost component breakdown for this example in Table XIII with the original breakdown using the previous set of pre-selected contingencies shows that the proportions of the expected cost components have shifted toward the post-contingency control actions.

III. IEEE RTS STUDY

Here the stochastic market-clearing scheme is tested over a 24-h horizon on the IEEE RTS [2] shown in Fig. 4. This system contains 32 generators, each submitting offers to produce energy consisting of four incremental cost/power blocks [2, Table 9]. These offers hold for each hour of the horizon and are based on the fuel costs found in Table XIV [12]. The upper limit of block 1 is considered as the minimum power output of the thermal generators. In addition, the startup costs are the “cold” values given in [2, Table 8]. Ramp rates, minimum up, and down times are as listed in [2, Table 10]. The up, down, startup, and shutdown ramps are all equal. The generator and line failure rate data are found, respectively, in [2, Tables 6 and 12]. Lastly, we assume that the nuclear (U400) and hydro (U50) generators are must-run units.

The hourly demand data correspond to Tuesday of Week 45, Winter Week Day, for the peak load of 2850 MW, while the spatial demand distribution corresponds to that of [2, Table 5]. The consumers are assumed to be inelastic. The value of lost load is equal to \$3000 per megawatthour for all buses during peak hours—hours 8 to 20 inclusive—while it is equal to \$2000 per megawatthour during the remaining off-peak hours. The loads offer spinning reserve, limiting their offers to 2% of their scheduled consumption for all hours and all buses. Both up and down demand-side spinning reserve services are offered at the rate of \$50 per megawatthour during the entire scheduling horizon.

Given the size of this problem, the pre- and post-contingency generator on/off variables are set to be equal; therefore, nonspinning reserve services are not available. Moreover, we assume that the generators offer the maximum possible amount of up

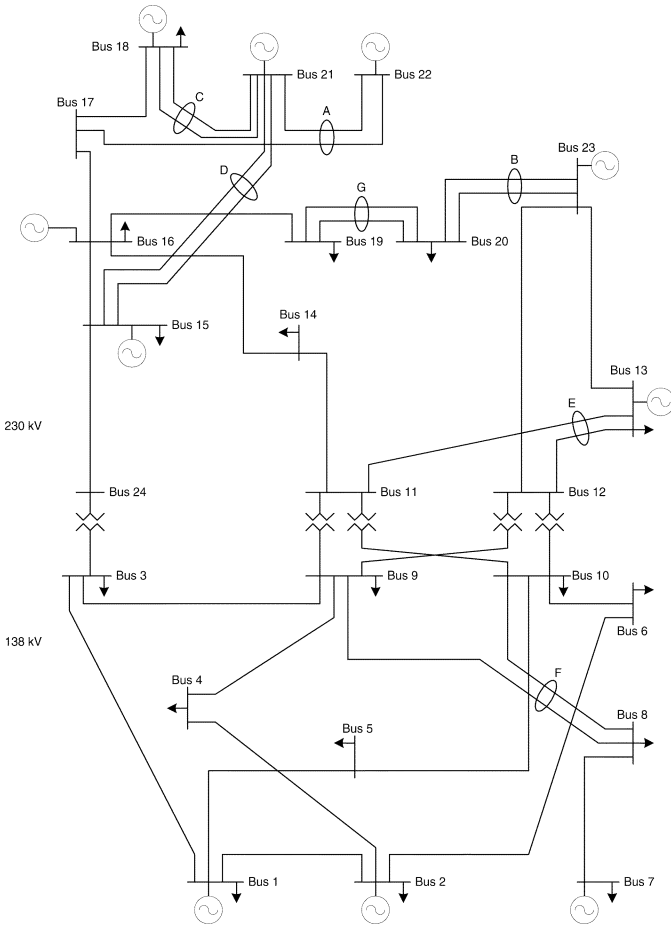


Fig. 4. IEEE RTS.

TABLE XIV
FUEL COST DATA (\$/MBTU)

Fuel	FO6	FO2	Coal	Nuclear
Cost	2.30	3.00	1.20	0.60

and down-going spinning reserve, both at a rate equal to 25% of their highest marginal cost of energy production.

The set of credible contingencies here consists of all generators having a capacity greater than or equal to 197 MW, specifically, the three U197 units located at bus 13, the U350 unit located at bus 23, and the two U400 units located at buses 18 and 21, respectively. This limited set is justified because it encompasses the contingencies with the most severe impact on the system-wide expected load not served [13].

Like the small-scale study, this case was solved using the mixed-integer linear programming solver CPLEX 9.0.2 under GAMS [3]. With a pre-specified duality gap of 1%, the CPU solution time was 40 minutes and 41 seconds on a Linux-based server with 1.60-GHz processors and 2 GB of RAM. The dimensions of the model are noteworthy: 1 018 033 variables—576 of which are binary¹—and 1 754 981 constraints. A breakdown of the main contributors to the formulation's

¹The number of binary variables reflects the fact that eight of the generators (U50 and U400) were assumed to be must-run. Moreover, we did not use extra binary variables to model the startup and shutdown of the units. This saving is, however, reflected in an increase in the number of constraints [14].

TABLE XV
BREAKDOWN OF THE DOMINANT VARIABLE AND CONSTRAINTS—POST-CONTINGENCY

Variable	Count
Voltage angles	43,200
Load shedding	43,200
Net power output	340,224
Power blocks	428,544
Constraint	Count
Power balance	43,200
Sum over the power blocks	107,136
Power flow limits	273,600
Upper bounds on power blocks	428,544

TABLE XVI
COMPARISON OF EXPECTED COSTS (\$)—DETERMINISTIC VERSUS STOCHASTIC

	Pre-contingency	Reserve deployment	Loss-of-load
Deterministic	379,540	56,602	0
Stochastic	379,382	52,298	161
Difference	158	4304	-161

variable and constraint counts is given in Table XV. We point out that the numbers quoted here are those of the formulation before the pre-processing engine of CPLEX is run, whose role is to remove redundant constraints (rows) and optimization variables (columns). Thus, after pre-processing, the problem array size is reduced to 383 276 rows and 297 079 columns, representing a more reasonable problem size. Examples of redundant variables include the voltage angle of the reference bus, which is always fixed, or the pre-contingency load shedding variables, which should always be equal to zero. Likewise, redundant constraints include ramping limitations applying to generators, which are forced to stay offline because of minimum downtime restrictions imposed by the preceding scheduling horizon.

From the above, it is clear that, notwithstanding the relatively small size of the IEEE RTS, the dimensions of the corresponding stochastic market-clearing scheme are high. Nonetheless, some simplifications can be made to mitigate this dimensionality issue. For example, instead of representing the full grid, a zonal approach could be used, wherein only the transmission links between a restricted number of areas are modeled. Reducing the number of contingencies considered can also lower the dimensionality, under the philosophy that it is better to consider a few significant contingencies than none at all. In addition, as mentioned in the companion paper, the use of scenario reduction techniques [15]–[17] is promising, as are decomposition techniques based on Benders' decomposition [18]–[21] and “branch-and-price” decomposition [22]–[24]. Not to be neglected are the constant improvements in the cost and performance of computing machinery and optimization codes. These allowed the development of the current ISOs in the United States—something not conceivable 20 years ago.

Table XVI compares the breakdown of the expected cost of the optimal stochastic schedule to the expected cost of the deterministic schedule where load shedding is not permitted. Just

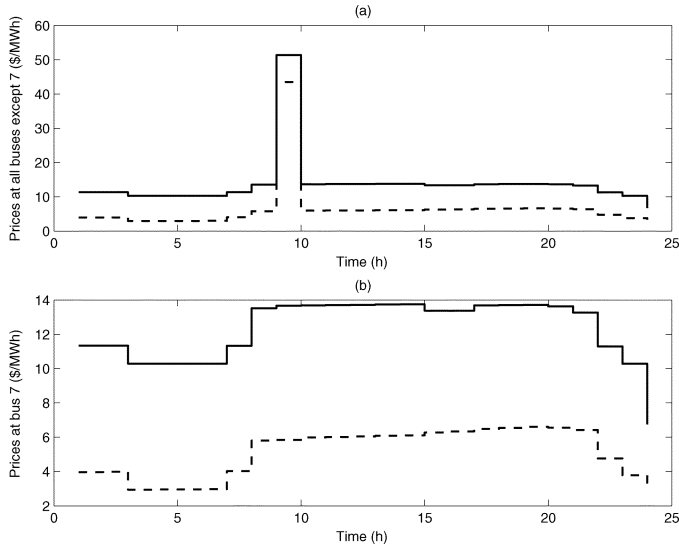


Fig. 5. Marginal prices of energy (solid line) and security (dashed line). (a) At all buses except bus 7. (b) At bus 7.

as in the previous case study, the expected cost of the deterministic schedule is calculated through (1). Table XVI shows that according to the stochastic schedule, the “Pre-contingency” and “Reserve deployment” expected costs, particularly the latter, are lower than the corresponding quantities under the deterministic schedule. These stochastic schedule benefits are slightly eroded by the expected cost of load shedding (\$161); however, when we consider all three effects, the stochastic solution provides a net expected benefit of \$4301. This is the VSS for this case study. Lastly, we point out that the expected load shedding in the stochastic schedule is applied at buses 8 and 20 (in the amount of 0.0404 MWh at each bus) during hour 1 when the value of lost load is at its lowest level.

For the stochastic schedule, Fig. 5(a) shows the time evolution of the marginal prices of energy and security at all buses except bus 7, while Fig. 5(b) shows how prices vary at bus 7. During hour 9, a significant price spike occurs raising security prices to \$43.46/MWh and energy prices to \$51.29/MWh, everywhere except at bus 7, where the prices remain at \$5.84/MWh for security and \$13.67/MWh for energy. This price spike arises from a number of factors. Referring to Fig. 4, during hour 9, the U100 generators located at bus 7 have plenty of cheap up-spinning reserve available; however, they are limited by the transmission limit (175 MW) imposed by the line linking this bus to the rest of the system. Also, during that hour, two out of the three U197 generators must be scheduled off because of a minimum down time constraint. Therefore, with so little capacity available, the operator is forced to *a*) turn on the four expensive U20 generators and *b*) schedule 1.71 MW of expensive demand-side up-spinning reserve at bus 13.

IV. CONCLUSION

In the second part of this two-paper series, we have examined examples of the market-clearing formulation with stochastic security proposed in the first companion paper.

In a small system case study, we assessed the impact on the stochastic generation and reserves schedules of *a*) line flow

limits, *b*) nonspinning reserve, *c*) demand-side value of load not served, *d*) ramping limits, and *e*) the pre-selected set of contingencies. Moreover, we compared the scheduling results of the proposed stochastic formulation with those obtained with a purely deterministic formulation in which involuntary load shedding is not allowed. The expected costs of preventive and corrective security control actions were found to be lower in the stochastic case. These savings were slightly diminished by the expected cost of involuntary load shedding.

In the stochastic approach, we also observed that the balance between security and cost is strongly impacted by the value placed by the customers on involuntary load shedding. In addition, the prices of energy and of security were calculated for the stochastic schedule and were compared to those corresponding to the deterministic schedule without load shedding. This comparison showed that with stochastic market-clearing, when load shedding is employed, the corresponding prices of energy and security are lower than those under the deterministic schedule. In essence, this means that as the risk of involuntary load shedding increases, the consumers pay less for security and energy.

The second case study ran a 24-h stochastic scheduling of the IEEE RTS. This study demonstrated that, for large-scale cases, care must be taken to restrict the number of pre-selected contingencies and their time of occurrence within the scheduling horizon. For instance, an inspection of the solution results showed that the vast majority of the constraints remain inactive, a property that warrants further investigation. We believe that solution techniques based on delayed constraint generation and Benders’ decomposition are promising strategies. These could keep the size of the constraint set required in the core memory to a more reasonable level while allowing for a larger degree of parallelism. The fact that many of the constraints are inactive also justifies the investigation of scenario reduction techniques for stochastic programs proposed in the literature. These aspects are currently under investigation.

Most importantly, however, these studies have underlined the potential economic benefits of a stochastic market-clearing formulation through the optimization of the expected costs of reserve deployment and involuntary load shedding.

APPENDIX

Consider the following security-constrained market-clearing problem, optimizing the cost function $C(\mathbf{u}, \mathbf{x})$

$$\min_{\mathbf{u}, \mathbf{x}} C(\mathbf{u}, \mathbf{x}) \quad (2)$$

subject to

$$\mathbf{h}(\mathbf{u}, \mathbf{x}) = \mathbf{0} \quad (\boldsymbol{\mu}_0) \quad (3)$$

$$\mathbf{h}(\mathbf{u}, \mathbf{x}, k) = \mathbf{0}; \quad k = 1, \dots, K \quad (\boldsymbol{\mu}_k) \quad (4)$$

$$\mathbf{g}(\mathbf{u}, \mathbf{x}) \geq \mathbf{0} \quad (\boldsymbol{\sigma}) \quad (5)$$

where the vectors \mathbf{u} and \mathbf{x} represent, respectively, all discrete and continuous variables. The vector constraint (3) represents the power balance under the noncontingent scenario, while (4) represents the power balance conditions for each of the pre-selected $k = 1, \dots, K$ failure scenarios. The vector inequality (5)

lumps all the remaining constraints. Associated with their respective constraints (3)–(5) are the Lagrange multiplier vectors $\boldsymbol{\mu}_0, \boldsymbol{\mu}_k; k = 1, \dots, K$ and $\boldsymbol{\sigma}$.

The formulation of the companion paper [1] is a specific implementation of the above mathematical program, where the contingency scenarios are indexed such that $k \equiv (k, \tau)$.

Given an optimal solution $(\mathbf{u}^*, \mathbf{x}^*)$ to (2)–(5), under smoothness assumptions and while keeping the discrete variables fixed at \mathbf{u}^* , the marginal costs of energy and security at the optimal solution are, respectively,

$$\frac{\partial C}{\partial \mathbf{E}} = \boldsymbol{\mu}_0 + \sum_{k=1}^K \boldsymbol{\mu}_k, \quad (6)$$

and

$$\frac{\partial C}{\partial \mathbf{S}} = \sum_{k=1}^K \boldsymbol{\mu}_k \quad (7)$$

where $d\mathbf{E}$ represents an incremental vector perturbation of the power balance relations under the noncontingent state (3), and $d\mathbf{S}$ is a supplementary incremental perturbation of the power balance relations in the failed states (4). Therefore, under marginal pricing, (6) and (7) become, respectively, the nodal prices of energy and security. We refer the reader to [7] for a proof.

REFERENCES

- [1] F. Bouffard, F. D. Galiana, and A. J. Conejo, "Market-clearing with stochastic security—Part I: Formulation," *IEEE Trans. Power Syst.*, vol. 20, no. 4, pp. 1818–1826, Nov. 2005.
- [2] Reliability Test System Task Force, "The IEEE reliability test system—1996," *IEEE Trans. Power Syst.*, vol. 14, no. 3, pp. 1010–1020, Aug. 1999.
- [3] A. Brooke, D. Kendrick, A. Meeraus, and R. Raman, *GAMS: A User's Guide*. Washington, DC: GAMS Development Corp., 2003.
- [4] J. R. Birge and F. Louveaux, *Introduction to Stochastic Programming*. New York: Springer-Verlag, 1997.
- [5] F. C. Schweppe, M. C. Caramanis, R. D. Tabors, and R. E. Bohn, *Spot Pricing of Electricity*. Boston, MA: Kluwer, 1988.
- [6] X. Ma, D. I. Sun, and K. W. Cheung, "Evolution toward standardized market design," *IEEE Trans. Power Syst.*, vol. 18, no. 2, pp. 460–469, May 2003.
- [7] J. M. Arroyo and F. D. Galiana, "Energy and reserve pricing in security and network-constrained electricity markets," *IEEE Trans. Power Syst.*, vol. 20, no. 2, pp. 634–643, May 2005.
- [8] T. Alvey, D. Goodwin, X. Ma, D. Streiffert, and D. Sun, "A security-constrained bid-clearing system for the New Zealand wholesale electricity market," *IEEE Trans. Power Syst.*, vol. 13, no. 2, pp. 340–346, May 1998.
- [9] K. W. Cheung, P. Shamsollahi, D. Sun, J. Milligan, and M. Potishnak, "Energy and ancillary service dispatch for the interim ISO New England electricity market," *IEEE Trans. Power Syst.*, vol. 15, no. 3, pp. 968–974, Aug. 2000.
- [10] S. M. Shahidehpour, H. Yamin, and Z. Li, *Market Operations in Electric Power Systems: Forecasting, Scheduling, and Risk Management*. New York: IEEE, 2002.
- [11] T. Wu, M. Rothleder, Z. Alaywan, and A. D. Papalexopoulos, "Pricing energy and ancillary services in integrated market systems by an optimal power flow," *IEEE Trans. Power Syst.*, vol. 19, no. 1, pp. 339–347, Feb. 2004.
- [12] R. Billinton and W. Li, *Reliability Assessment of Electric Power Systems Using Monte Carlo Methods*. New York: Plenum, 1994.
- [13] R. Billinton and R. Mo, "Deterministic/probabilistic contingency evaluation in composite generation and transmission systems," in *Proc. IEEE Power Engineering Society General Meeting*, Denver, CO, 2004, pp. 2232–2237.

- [14] M. C. Ruiz-Peinado, "Coordinación Hydrotérmica Mediante Programación Lineal Entera-Mixta," Tech. Rep., E.T.S.I. Industriales, Univ. de Castilla-La Mancha, Ciudad Real, Spain, 2003.
- [15] J. Dupačová, N. Gröwe-Kuska, and W. Römisch, "Scenario reduction in stochastic programming: An approach using probability metrics," *Math. Program., Ser. A*, vol. 95, pp. 493–511, Mar. 2003.
- [16] H. Heitsch and W. Römisch, "Scenario reduction algorithms in stochastic programming," *Comput. Optim. Appl.*, vol. 24, pp. 187–206, Feb. 2003.
- [17] N. Gröwe-Kuska, H. Heitsch, and W. Römisch, "Scenario reduction and scenario tree construction for power management problems," in *Proc. IEEE PowerTech.*, vol. 3, Bologna, Italy, 2003.
- [18] J. F. Benders, "Partitioning procedures for solving mixed-variables programming problems," *Numer. Math.*, vol. 4, pp. 238–252, 1962.
- [19] D. Bertsimas and J. N. Tsitsiklis, *Introduction to Linear Optimization*. Belmont, MA: Athena Scientific, 1997.
- [20] H. Ma and S. M. Shahidehpour, "Unit commitment with transmission security and voltage constraints," *IEEE Trans. Power Syst.*, vol. 14, no. 2, pp. 757–764, May 1999.
- [21] Z. Li and M. Shahidehpour, "Security-constrained unit commitment for simultaneous clearing of energy and ancillary services markets," *IEEE Trans. Power Syst.*, vol. 20, no. 2, pp. 1079–1088, May 2005.
- [22] C. Barnhart, E. L. Johnson, G. L. Nemhauser, M. W. P. Savelsbergh, and P. H. Vance, "Branch-and-price: Column generation for solving huge integer programs," *Oper. Res.*, vol. 46, pp. 316–329, May/June 1998.
- [23] F. Vanderbeck, "On Dantzig-Wolfe decomposition in integer programming and ways to perform branching in a branch-and-price algorithm," *Oper. Res.*, vol. 48, pp. 111–128, Jan./Feb. 2000.
- [24] G. Lulli and S. Sen, "A branch-and-price algorithm for multistage stochastic integer programming with application to stochastic batch-sizing problems," *Manage. Sci.*, vol. 50, pp. 786–796, Jun. 2004.



François Bouffard (S'99) received the B.Eng. (Hon.) degree in electrical engineering from McGill University, Montreal, QC, Canada, in 2000. He is currently working toward the Ph.D. degree at McGill University.

He was recently a Visiting Scholar at the Universidad de Castilla-La Mancha, Ciudad Real, Spain, and a Faculty Lecturer in the Department of Electrical and Computer Engineering, McGill University. His research interests are in the fields of power systems economics, reliability, control, and optimization.



Francisco D. Galiana (F'91) received the B.Eng. (Hon.) degree from McGill University, Montreal, QC, Canada, in 1966 and the S.M. and Ph.D. degrees from the Massachusetts Institute of Technology, Cambridge, in 1968 and 1971, respectively.

He spent some years at the Brown Boveri Research Center, Baden, Switzerland, and held a faculty position at the University of Michigan, Ann Arbor. He joined the Electrical Engineering Department of McGill University in 1977, where he is currently a Full Professor.



Antonio J. Conejo (F'04) received the M.S. degree from the Massachusetts Institute of Technology, Cambridge, in 1987, and a Ph.D. degree from the Royal Institute of Technology, Stockholm, Sweden, in 1990.

He is currently a Full Professor at the Universidad de Castilla-La Mancha, Ciudad Real, Spain. His research interests include control, operations, planning, and economics of electric energy systems, as well as statistics and optimization theory and its applications.